Appl. Phys. A 73, 467–475 (2001) / Digital Object Identifier (DOI) 10.1007/s003390100781

Applied Physics A
Materials
Science & Processing

Positron annihilation studies on the migration of deformation induced vacancies in stainless steel AISI 316 L

U. Holzwarth[1,*], A. Barbieri[1], S. Hansen-Ilzhöfer[1], P. Schaaff[2], M. Haaks[3]

[1] European Commission, Joint Research Centre, Via E. Fermi 1 (T.P. 202), 21020 Ispra (VA), Italy
[2] Max-Planck-Institut für Metallforschung, Heisenbergstrasse 1, 70569 Stuttgart, Germany
[3] Institut für Strahlen- und Kernphysik der Universität Bonn, Nussallee 14–16, 53115 Bonn, Germany

Received: 11 August 2000/Accepted: 13 November 2000/Published online: 28 February 2001 – © Springer-Verlag 2001

Abstract. Positron lifetime measurements were carried out at room temperature before and after isochronous annealing of cylindrical, machined fatigue specimens and of round slabs of austenitic stainless steel AISI 316 L deformed in compression. Annealing experiments are evaluated in terms of vacancy migration and sinking to grain boundaries and dislocations. The model assumes spherical grains with a homogeneous initial distribution of vacancies. A vacancy migration enthalpy of $H_V^M = (0.9 \pm 0.15)$ eV was found. It is concluded that positron trapping at dislocation lines does not significantly contribute to positron lifetime measurements at room temperature and that single vacancies are the dominating positron traps. Positron annihilation depth profiling on cross-sectional areas prepared from machined specimens using a positron microprobe with 10 μm spatial resolution shows that machining of cylindrical specimens creates vacancies up to 5 mm below the surface.

PACS: 61.72.-y; 61.72.Hh; 78.70.Bj; 81.70.-q

The present investigation of vacancy migration in stainless steel AISI 316 L was motivated by a series of experiments to investigate the potential of positron-annihilation lifetime measurements as a non-destructive testing method in mechanical engineering. For such an investigation the purely austenitic stainless steel AISI 316 L is a suitable material because it has been studied extensively for nuclear energy applications. It remains a single phase austenitic material under all application conditions relevant to this study. Therefore, the evaluation of positron-lifetime measurements during plastic deformation does not need to consider deformation induced phase transformations. Annealing experiments, carried out in order to investigate machining damage on the cylindrical fatigue specimens and to separate the effects of positron trapping into dislocations and vacancies, were exploited to derive data on vacancy migration properties. Such data are rare in literature because solid state physics focuses on simple alloys, e.g. to study vacancy–impurity interactions in dilute iron alloys [1, 2]. On the other hand, the ongoing development of special-purpose steels leads to an increasing diversity of chemical composition. For instance, the present AISI 316 L material stems from a general purpose 18 wt % Cr–8 wt % Ni stainless steel whose corrosion resistance was improved by alloying with molybdenum. The necessity to improve its welding characteristics for nuclear applications led to a reduction in the carbon content [3]. Hence, the "L" stands for "low carbon". The stainless steel AISI 321, for which some reference data concerning the vacancy migration exist, has an additional alloying content of 0.5 wt % titanium to prevent carbide precipitation [3]. Ehrhart [1] summarized the knowledge on atomic defects in face-centered cubic Cr-Fe-Ni solid solution and austenitic steels. Little is precisely known and basic investigations were made on model alloys kept free from minor alloying contents such as carbon, nitrogen or silicon and are usually free of the complex microstructures that characterize complex steels [4]. For stainless steel AISI 316, it is however known that vacancy migration starts at slightly lower temperature than for the pure Cr-Fe-Ni solution [1, 4]. This means that vacancy trapping by minor alloying components may be neglected in stainless steel [1, 4], in contrast to pure α-iron, where a strong interaction of vacancies with an even small content of an interstitial impurity such as carbon is reported [5].

A further challenge is posed by the evaluation of the annealing experiments. Dryzek et al. [6] pointed out that simple first-order kinetics, which has successfully been applied to describe the annealing in irradiated iron and iron alloys, leads to unphysically low activation enthalpies for the elementary annealing process if it is applied to plastically deformed metals. Therefore, these authors adopted the solution of the diffusion problem in a sphere, which can be applied to describe the outgassing or the uptake of a solute from or by a sphere [7], and applied it successfully to vacancy migration in deformed polycrystals [6, 8]. The model, outlined in Sect. 1.3, has been used in the present work.

The principle experimental set-up of a $^{72}Se/^{72}As$ positron generator for non-destructive measurements has already been presented [9], as have first results on in situ positron-

*Corresponding author.
(Fax: +39-0332-785388, E-mail: uwe.holzwarth@jrc.it)

lifetime measurements during fatigue of stainless steel AISI 316 L [10]. The comparison of experiments at different stress amplitudes was however disturbed by a pronounced variability of the initial mean positron lifetime of the specimens, ranging between 118 ps and 137 ps, with a preference for values above 130 ps. On the other hand, in the centre of several carefully prepared cross-sectional specimens, positron lifetimes of (108 ± 3) ps were always found; they were attributed to positron annihilation in the perfect lattice. The observed variation of the initial positron lifetimes measured on the cylindrical gauge length might be an effect of the production procedure by machining. It is known that stainless steels require greater power and lower machining speed compared to carbon and low-alloy steels due to their higher strength and higher work hardening capability [3]. This reduces the service life of tools and causes machining damage, giving rise to internal stresses and defects in the surface layer. Since the penetration depth of positrons with the most frequent energies in the β^+-spectrum of the ^{72}Se/^{72}Ge generator is about 350–500 μm [9, 11], the initial state may partially mask the very early fatigue-induced microstructure changes to be investigated in our experiments. A thermal pre-treatment does, however, not solve the problem because there is strong evidence that vacancies are the major positron traps even at high dislocation densities and that annealing of dislocations occurs at temperatures where also carbides precipitate.[1]

The interpretation of the results is based on recent experimental [11, 12] and theoretical [13–15] evidence for copper, aluminum and iron that positrons are not directly trapped by dislocations at room temperature since their dilatation zones are traps that are too shallow. Gauster et al. [16] studied the fatigue damage evolution of cold-rolled stainless steel 316 L by positron-annihilation line shape analysis and concluded that trapping to dislocations in this stainless steel is very low or the annihilation properties in dislocations are very similar to those of the bulk. These authors found no correlation between their *S*-parameter measurements and the dislocation density determined by transmission electron microscopy (TEM) after fatigue at different stress amplitudes and fatigue temperatures. Isochronous annealing experiments were performed on specimens deformed by cold-rolling to a 25% thickness reduction in order to separate the vacancy and dislocation contributions to the *S*-parameter measurements. The experiments, which were accompanied by TEM and Knoop microhardness measurements, showed that annealing starts around 430 K but no dislocation annealing occurred below 873 K [16]. Thus, deformation induced microstructural changes are probed by positrons at room temperature via vacancies which are produced by various dislocation processes during plastic deformation. Hence, positron-lifetime measurements after isochronous annealing treatments in the temperature range between 430 K and 873 K, in which the dislocation density is not subjected to significant changes, should give quantitative information to identify the positron trapping defect.

These findings are not in contradiction to evidence for direct positron trapping to dislocations if positron annihilation is measured at temperatures sufficiently low to suppress thermally activated detrapping. In positron-lifetime measurements carried out at 77 K on pure α-iron, Park et al. [17] and Hidalgo et al. [18] could identify positron traps with a specific positron lifetime of about 150 ps, which they attributed to annihilation events in the dilatational zone around dislocations. Most of the more recent experimental (e.g. [18–21]) and theoretical (e.g. [13]) examinations agree however that dislocations are traps too shallow to effectively bind positrons at room temperature.

[1] Since the specimens were to be used for further fatigue testing, solution annealing and quenching could not be applied in order to avoid distortions and other shape changes of the specimens.

1 Experimental procedures and evaluation

1.1 Material and specimen preparation

The base material were large stainless steel AISI 316 L plates of 30 mm thickness. The material composition as specified by the supplier, Creusot–Loire, is given in Table 1. The plates were hot rolled, solution annealed at 1050 °C for 30 min in order to dissolve carbides and then quenched by submersion of the plates in cold water. According to the chromium and nickel equivalents calculated after Pryce and Andrews [22], the content of ferrite is about 1% only. Metallography shows that the ferrite is localized in stringers parallel to the rolling direction of the material. The grain size of the material has been determined according to ASTM E112-88 [23] by the linear intercept method and was found to be 40 μm. From these plates bars of 30 mm × 30 mm × 170 mm were cut by spark erosion and cylindrical fatigue specimens were fabricated by machining with tangentially blending fillets between the gauge length and the gripping parts. The gauge length with a diameter of 10 mm was 30 mm long. On the gripping part, the specimens had a diameter of 20 mm. This specimen shape and the way of executing the fatigue tests corresponds to the ASTM Standard E466-82 [23] for "Conducting Constant Amplitude Axial Fatigue Tests of Metallic Materials".

The residual concentration of vacancies due to solution annealing and quenching can be considered as low in spite of the annealing temperature of 1050 °C corresponding to 78% of the melting temperature of stainless steel AISI 316 L of 1425 °C [24]. A theoretical estimate based on a typical vacancy concentration of 5×10^{-4} in thermodynamic equilibrium at the melting point [25] and a vacancy formation enthalpy $H_V^F = 1.61$ eV [1] yields an equilibrium concentration at the annealing temperature of about 2×10^{-5}. The expected cooling rate achievable by water quenching[2] in the center part of a 30 mm thick plate, where the specimens stem from, is however low due to the low thermal conductivity of stainless steel (13.95 W m^{-1} K^{-1} [24]). Thus, only a few percent

[2] Water quenching is applied to avoid the re-creation of carbides by the migration of carbon atoms in the austenitic matrix.

Table 1. Chemical composition of stainless steel AISI 316 L according to supplier certificate

elements	C	Si	Mn	Ni	Cr	Mo	S	P	Fe
weigth-%	0.018	0.582	1.676	11.13	17.38	2.151	0.002	0.021	67.04
at.-%	0.08	1.15	1.69	10.53	18.57	1.24	0.01	0.04	66.68

of the equilibrium concentration will be preserved. The concentration of vacancies in an Fe-Cr-Ni alloy after quenching from 1050 °C has been estimated by Wang et al. [26] to be about 10^{-6}.

For first screening the positron lifetime of several fatigue specimens was measured before and after thermal annealing treatments. The thermal treatments were performed at various temperatures between 348 K and 1075 K in a pure argon atmosphere. The specimens were heated up in the furnace, kept at temperature for 60 min and then cooled in an argon atmosphere.[3] Due to the large mass of the specimens and the low thermal conductivity of stainless steel, the annealing time–temperature profile was not precisely defined.

In order to have precisely defined annealing times and temperatures, two fatigue specimens were sacrificed and the gauge lengths were sliced by spark erosion in slabs of 10 mm diameter and 3.1 mm height. The positron lifetimes measured in the centre of the slabs were in the range (108 ± 3) ps. Hence, no further steps were undertaken to improve the surface quality after cutting by spark erosion. Two groups of slabs were prepared with 10% and 20% thickness reduction. In these cases forces up to 55 kN and 92.5 kN had to be applied, which correspond to nominal compression stresses of 700 MPa and 1175 MPa, respectively. The specimens were then inserted in a pre-heated furnace, kept at the desired temperatures for 60 min, then removed from the furnace and quenched in oil. A small mass, a higher surface-to-volume ratio and quenching in oil assured a much better time control of the thermal treatments. The upper limit for the annealing temperature was chosen as 673 K according to the results on the entire cylindrical fatigue specimens presented in Fig. 1. The new increase of the positron lifetime above 800 K can be explained by the formation of carbides which introduce new trapping sites and complicate the interpretation of the positron annihilation measurements.

1.2 Positron lifetime measurements

The mobile positron beam used for the present experiments has already been described in detail [9, 11]. It is based on a $^{72}Se/^{72}As$ positron generator with a 0.6 mm diameter which is collimated by a little gold tube of 0.6 mm inner and 2 mm outer diameter and about 1.2 mm length which is integrated in the tip of a plexiglass light guide on top of a photomultiplier tube. The collimated source is covered by a plastic scintillator which produces a scintillation start signal only for those positrons which are emitted in the direction of the specimen under examination. The set-up is shielded against light by a 12 μm thick aluminum foil. A specimen at a distance of 3 mm from the end of the collimator is subjected to positron irradiation in an area of 3.6 mm in diameter. The stop signal is delivered by a BaF_2 crystal after registration of the 511 keV annihilation quanta. Signal processing is done by a fast–slow coincidence measurement as described in [9, 11].

The specimens were surrounded by a plexiglass shielding which captured all positrons missing the specimen or being reflected from its surface. The mean positron lifetime in plexiglass of about 1500 ps is sufficiently different from the mean positron lifetimes expected in a metal of 100–200 ps that an easy background correction can be performed by weighted subtraction of a plexiglass reference spectrum. The weighting factor is determined from the ratio of counts in a window of the spectrum to be analyzed, in which the spectrum is determined only by very long-lived contributions, and in a reference spectrum registered when the specimen was replaced by plexiglass dummy. For the background correction the width of the windows and their position with respect to the centers of the annihilation spectra were identical. Before correction each spectrum contained 1.1×10^6 coincidence events. Typically 55% of these events were lost by the weighted subtraction of the reference spectrum. The average positron lifetime is then evaluated by a weighted linear regression to the linear part of the spectrum (logarithmic presentation).[4] This method also corrects for the annihilation events of low energy positrons in the scintillation start detector and the aluminum foil shielding the photomultiplier tube from daylight.

The time resolution of the instrument was determined as the full width at half maximum of the 835 keV prompt (3 ps) line emitted from the ^{72}Ge after the emission of a 2.5 MeV positron by the ^{72}As. Alternatively, a Gaussian curve was fitted to the prompt line. Both methods yield a time resolution of (230 ± 5) ps.

1.3 Evaluation of annealing experiments

For the evaluation of the annealing experiments, a model recently presented by Dryzek et al. [6, 8] was applied. It is based on the assumption that (a) grain boundaries and dislocations are the dominating sinks for migrating vacancies. For simplicity of the mathematical description, it is further assumed (b) that the grains are approximately of spherical shape with (c) an initially homogeneously distributed concentration of vacancies and (d) that the sinks are not significantly modified by absorption of vacancies. The initial content of vacancies in the grains will gradually fade away when vacancies

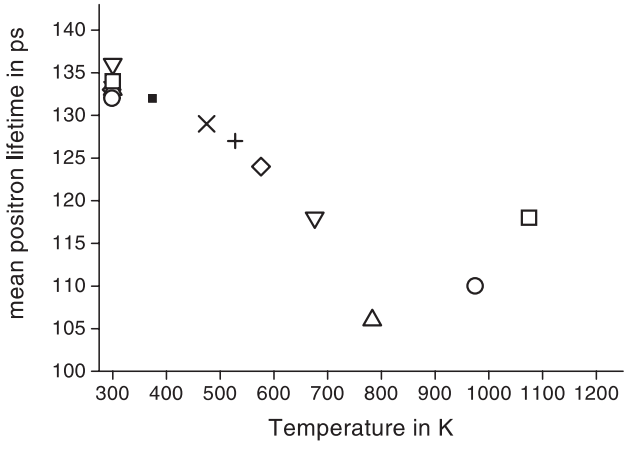

Fig. 1. Mean positron lifetimes of machined fatigue specimens initially determined at 300 K and after annealing for 60 min at the indicated temperatures. Identical symbols belong to the same fatigue specimens

[3] In this case quenching could not be applied in order to avoid distortions of the cylindrosymmetric specimens to be used in further fatigue experiments.

[4] A systematic decomposition of the mean positron lifetime into different components has not yet been performed, since at least twice the number of coincidence events are recommended for a stable decomposition in more lifetime components [27]. Moreover, additional experimental techniques would be required to gain further information on the configuration of large vacancy clusters.

become mobile. The presence of dislocations in the grains is dealt with by regarding the grain radius as an effective radius which is smaller than the metallographically determined one. For the case of radial diffusion in a sphere, the concentration changes can be calculated [7, 28] according to

$$\frac{c_0(t,T)}{c_0} = \frac{6}{\pi^2}\sum_{k=1}^{\infty}\frac{1}{k^2}\exp\left(-D(T)\frac{k^2\pi^2 t}{R^2}\right) \quad , \tag{1}$$

where k is an integer, R stands for the effective grain radius and $D(T)$ is the diffusion constant of vacancies, given by

$$D(T) = D_0 \exp\left(-\frac{H_{\mathrm{M}}^{\mathrm{V}}}{k_{\mathrm{B}}T}\right) \quad . \tag{2}$$

Here, $H_{\mathrm{M}}^{\mathrm{V}}$ denotes the migration enthalpy of a vacancy, D_0 the pre-exponential diffusion constant and k_{B} the Boltzmann constant.

The vacancy concentration from the mean positron lifetime was calculated after the trapping model by Bergersen and Stott [29] and Connors and West [30]. This model considers only annihilation events of free positrons in the flawless lattice and those in one type of trap, which is assumed to be a single vacancy. If τ_{L} denotes the positron lifetime in the flawless lattice and τ_{V} the positron lifetime in vacancies present in the concentration c and trapping positrons with a rate μ, the mean positron lifetime can be obtained as

$$\tau(t,T) = \tau_{\mathrm{L}} \cdot \frac{1+\tau_{\mathrm{V}}\mu c}{1+\tau_{\mathrm{L}}\mu c} \quad . \tag{3}$$

From two measurements of the mean positron lifetime, τ_0 before and $\tau(t,T)$ after an annealing experiment at temperature T for a time t, we can calculate the left-hand part of (1) as

$$\frac{c(t,T)}{c_0} = \frac{(\tau(t,T)-\tau_{\mathrm{L}})\cdot(\tau_{\mathrm{V}}-\tau_0)}{(\tau_{\mathrm{V}}-\tau(t,T))\cdot(\tau_0-\tau_{\mathrm{L}})} \quad . \tag{4}$$

In this way the pre-exponential factor D_0 and the migration enthalpy of vacancies $H_{\mathrm{M}}^{\mathrm{V}}$ can be derived from a numerical fit of the model to the positron lifetime measurements, provided grain boundaries and dislocations are the dominating sinks for vacancies and that the specific positron lifetimes in the flawless lattice and the vacancies are known.

The only feasible way to deal with vacancy sinking to dislocations is to consider the spherical grain radius R as an effective value and adjustable parameter in the fit procedure. Sinking along dislocations will lead to values for R smaller than the metallographic grain radius. A TEM study of the microstructure after compression of the stainless steel slabs was not performed, since the geometry of the dislocation arrangement cannot indicate the sink strength of dislocations for vacancies. Various cases are conceivable which cannot be addressed by TEM. From molecular dynamics calculations and electron theory, one has to conclude that a positron trapped in a jog on an edge dislocation in a face-centered cubic material exhibits nearly the same positron lifetime as in a vacancy [13]. The same is valid for vacancies trapped in the strain field around a dislocation line or in the stacking fault area between two Shockley partial dislocations [13]. Thus, a vacancy moving to an edge dislocation can create another type of positron trap which is indistinguishable in our measurements from its free state. A vacancy moving to a pre-existing jog may move the jog along the dislocation line and one trapping site is lost. Other possibilities can be imagined, all having the same disadvantage that the available tools for microstructure investigations, such as TEM, do not deliver functional information on the sink strength of dislocations.

The fit was performed with the advanced curve fit option in ORIGIN[5] (Microcal Software Inc.) version 5.0 which uses a Levenberg–Marquart algorithm. The convergence and the stability of the fit was however unsatisfactory when all three parameters $H_{\mathrm{V}}^{\mathrm{M}}$, D_0 and R were fitted simultaneously. This problem was overcome by searching the best values of D_0 and R for constant migration enthalpy of vacancies $H_{\mathrm{V}}^{\mathrm{M}}$. $H_{\mathrm{V}}^{\mathrm{M}}$ was varied manually in steps of 0.01 eV in the range between 0.65 eV and 1.25 eV. The best fits were chosen from the smallest χ^2 sum for the triples ($H_{\mathrm{V}}^{\mathrm{M}}$, D_0, R), considering the physical relevance of the data, e.g., triples with R values above the metallographic grain size were excluded.

1.4 Machining damage investigations

Cross-section specimens were prepared from the gripping parts of the cylindrical stainless steel specimens of 20 mm diameter. The material was cut from the entire specimen by spark erosion, embedded in metallographic resin and carefully polished in several steps ending up with 1 μm diamond grade. After this procedure the severe damage from cutting was removed and the slight damage introduced by polishing extends according to our experience up to about 10 μm below the polished surface. This residual damage was not removed by electrochemical polishing in order to avoid the risk of possible hydrogen uptake, which could interact with positron traps and change their annihilation characteristics.

On such specimens a Vickers microhardness profile was measured. At sufficient distance from the microhardness indentations, Doppler broadening measurements of the 511 keV annihilation line were carried out with the positron microprobe at Bonn University [31, 32]. This instrument combines a scanning electron microscope (SEM) with a slow positron microbeam of variable energy up to 30 keV and a positron spot size of about 10 μm [31, 32]. The spot size determines the spatial resolution of the method. It allowed SEM imaging of the cross-section area of our specimens and in a second step the positron beam to be focused on a small spot close to the microhardness indentations, but sufficiently distant to exclude disturbing effects from the deformed zone around the hardness indentations on the positron annihilation measurements.

The penetration depth of the 30 keV positrons from the microprobe in steels is 1.2 μm. Therefore, with the present specimen preparation, the positron microprobe has to reveal the machining damage, which declines from the border to the centre of the cross-section specimens, on the background of a homogeneous damage caused by mechanical polishing. This was considered feasible in view of the successful monitoring of fatigue damage evolution on the cylindrical surfaces of the fatigue specimens [10] though machining caused damage yielded an initial offset of about 15–20 ps with respect to the defect free lattice.

In this way two profiles were obtained characterizing the mechanical properties by Vickers hardness numbers and

the density of vacancy-like positron-trapping defects by the *S*-parameter. The *S*-parameter characterizes the shape of the 511 keV positron annihilation line and is defined as the ratio of the area of a suitably chosen central part of the 511 keV γ line and the total area of the annihilation line. The method requires the registration of the 511 keV line with a Ge detector of sufficient energy resolution. With an increasing fraction of positrons trapped, e.g., in vacancies, the Doppler broadening of the annihilation line is reduced and *S* increases.

Both profiles were recorded before and after thermal treatment of the specimen at 350 °C for 20 h, which can be considered as sufficient to remove all vacancies in the material.

2 Results

2.1 Thermally activated migration of vacancies

Figure 1 shows the results of the positron-lifetime measurements on the cylindrical machined specimens before and after annealing at the given temperatures. As indicated in Sect. 1.1 the large specimens pose problems for the execution of thermal treatments with well-defined duration. However, from Fig. 1 it can be concluded that for temperatures above 800 K new positron trapping sites are created which are considered in the literature as chromium-rich $M_{23}C_6$ carbides [6, 33]. The orientation relationship $\{111\}\langle 110\rangle M_{23}C_6 || \{111\}\langle 110\rangle$austenite gives rise to a misfit of 0.013 [33] between the carbides and the austenitic host lattice, which favours the presence of misfit dislocations and associated defects. Since this effect may be expected in austenitic stainless steels at temperatures as low as 700 K [33, 34], the temperature range for isochronous annealing on the slabs deformed in compression was confined to temperatures up to 673 K.

Positron lifetime measurements after compression of the slabs gave rather reproducible results. After thickness reduction of 10% and 20%, positron lifetimes of 150 ps and 161 ps were determined, respectively, with a standard deviation of 3 ps. Within the accuracy of our measurements, both sets of specimens gave identical results concerning the positron lifetime changes after annealing and the calculated relative decrease of the vacancy concentration as shown in Figs. 2 and 3. The fit to the model (Fig. 3) outlined in Sect. 1.3 was performed with the merged data sets.

The error marks in Fig. 3 take into account the fact that the uncertainty in the determined mean positron lifetimes is ±3 ps due to thermal instabilities and drift effects of the photomultiplier tubes and the electronic system. This value was established by repeatedly recording a spectrum at constant microstructure over several days. The statistical error of the numerical fit of a mean positron lifetime to the background corrected spectrum is only ±0.5 ps. The error marks also incorporate the uncertainty of the positron lifetimes in the perfect lattice and in a vacancy. Consultation of Table 2 shows that the values of τ_L and τ_V of 105 ps and 175 ps, respectively can only be considered to be accurate within ±5 ps. Under these conditions the vacancy migration enthalpy can be determined as $H_V^M = (0.9 \pm 0.15\,\text{eV})$. As can be seen from Table 3, D_0 ranges between $3 \times 10^{-5}\,\text{m}^2\,\text{s}^{-1}$ for the higher and $6 \times 10^{-7}\,\text{m}^2\,\text{s}^{-1}$ for the lower values of H_V^M. As expected,

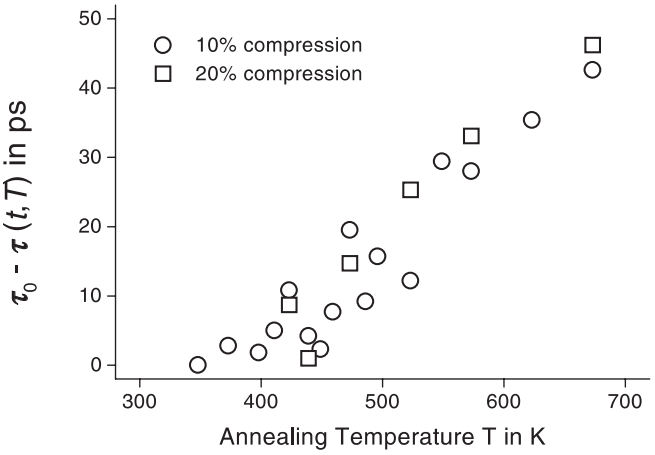

Fig. 2. Decrease of the mean positron lifetime τ after annealing for 60 min at annealing temperature T. Two sets of slabs are presented after 10% and 20% thickness reduction

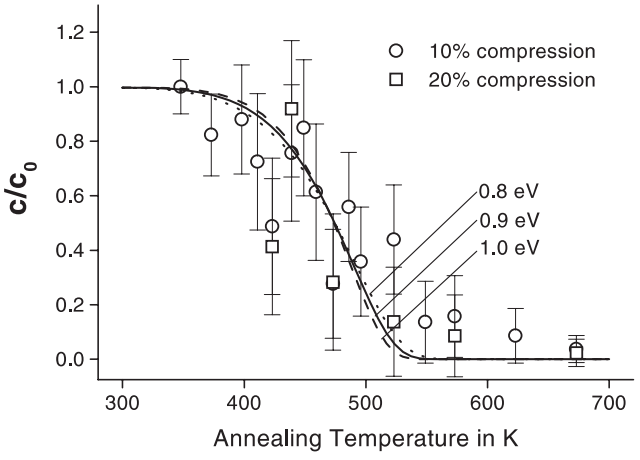

Fig. 3. Relative change of vacancy concentration c/c_0 after annealing at temperature T for 60 min. The lines are calculated using the fit parameters given in Table 3 for the three versions $H_V^M = 0.8$, 0.9 and 1.0 eV

the effective grain radius R is smaller than the metallographically determined one and ranges between 9 and 15 μm. Although the lowest χ^2 value was obtained for a vacancy migration enthalpy of 0.8 eV, and an effective grain radius of 15 μm, with the high dislocation density after a thickness reduction of 10% and 20%, let us assume that 9 μm may be more reasonable. Typical dislocation densities after such deformations are on the order of $1 \times 10^{14} - 1 \times 10^{15}\,\text{m}^{-2}$. Based on this consideration and the χ^2 sums, the parameter set (see Table 3) belonging to a vacancy migration enthalpy of 0.9 eV appears to be the more reasonable value.

2.2 Profile of machining damage

Figure 4 presents the results of the positron annihilation measurements across a carefully polished cross-section specimen and the corresponding microhardness values. Both measurements were performed before and after annealing the specimen at 350 °C for 20 h. From Fig. 4 it is evident that annealing affects only the Doppler broadening of the annihilation line, whereas the microhardness remains unchanged.

Table 2. Literature survey on positron lifetimes in the defect-free lattice (τ_L) and in vacancies (τ_V) in austenitic stainless steels, Fe-Cr-Ni alloys, α-iron and nickel

Source	Material	τ_L (ps)	τ_V(ps)
Lopes Gil et al. [35]	AISI 316		175
Hartley et al. [36]	AISI 304	100	
Dlubek et al. [37]	Ni	108	180
	Fe	105	175
Kamimura et al. [15]	Fe	110	176
Staab et al. [27]	Fe/Ni	104	
Schaefer [38]	Fe	106	176
Vehanen et al. [5]	Fe		175

Table 3. Fit results and χ^2 sums for the three curves presented in Fig. 3. In spite of the slightly higher χ^2 sum for the 0.9 eV set, the smaller effective grain size of 9 μm seems to be more reasonable due to the high dislocation density in the materials after plastic deformation

H_V^M (eV)	0.8	0.9	1.0
D_0 ($m^2\,s^{-1}$)	6×10^{-7}	2.5×10^{-6}	3×10^{-5}
R μm	15	9	9
χ^2	0.03322	0.03682	0.04014

This indicates that the applied annealing treatment does not introduce significant changes to the dislocation arrangement. The increase of the Doppler broadening parameter S towards the surface before annealing shows that the gradient of the concentration of trapping defects extends to about 5 mm below the surface. After annealing, the Doppler broadening parameter is constant throughout the cross-section and lower than the value initially measured in the centre of the specimen. This observation shows that annealing for 20 h at 350 °C removes practically all positron traps. Moreover, we conclude that the homogeneously distributed damage caused by mechanical polishing is not strong enough to significantly mask the machining damage which declines from the border towards the centre of the specimen. It is however not possible to state whether this machining damage penetrates even deeper than 5 mm into the material and whether it has a sharp border or declines smoothly.

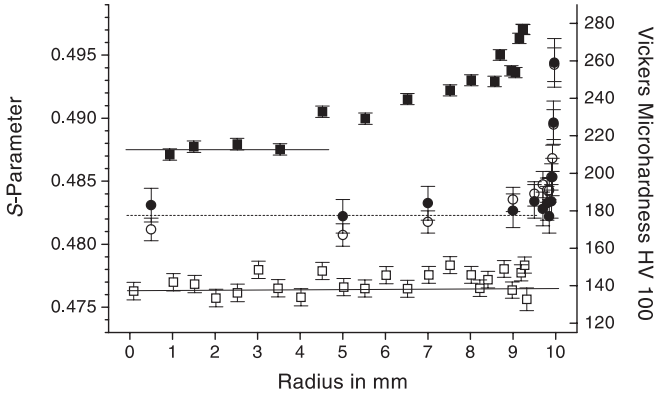

Fig. 4. Profiles of the Doppler broadening line shape parameter S (□) and the Vickers microhardness number HV 100 (○) measured across a cross-section specimen prepared from the gripping part of a machined stainless steel AISI 316 L fatigue specimen (diameter 20 mm) before (*solid symbols*) and after (*open symbols*) annealing for 20 h at 350 °C. The penetration of machining damage is detectable up to 5 mm below the surface with positron annihilation, but only to about 0.5 mm with microhardness measurements. The bulk values are indicated by *horizontal lines*

The complete removal of vacancies without significant changes to the specimen microstructure, i.e., to the dislocation density, confirms that dislocation lines do not significantly contribute to positron trapping in AISI 316 L stainless steel at room temperature. The decrease of the bulk value of the S parameter by about 2%, as indicated by the horizontal solid lines in Fig. 4, has no corresponding feature in our positron lifetime measurements. The values measured in the centre of the cross-section specimens of (108 ± 3) ps and (104 ± 3) ps before and after annealing show a tendency for smaller values after annealing, which is however not significant. This may simply be explained by the estimated thickness of the layer damaged by mechanical polishing (about 10 μm) and the different penetration depths of the 30 keV positrons of the microprobe (1.2 μm) and from the $^{72}Se/^{72}As$ positron generator (300–500 μm) into steel. The positron-lifetime measurements are insensitive to such a thin damaged surface layer.

3 Discussion

The annealing measurements indicate the onset of pronounced annealing of vacancies at temperatures above 400 K. This agrees with the findings of Gauster et al. [16] on stainless steel AISI 316 L, with the positron-annihilation measurements of Lopes Gil et al. [35] on AISI 316 and with the S parameter measurements of Dryzek et al. [6] and Haaks et al. [31] on stainless steel AISI 321. Dryzek et al. [6] also observed an increase of positron trapping defects after annealing at temperatures above 800 K. Dlubek et al. [37] investigated an austenitic stainless steel with a composition close to our material (in 18.45 wt % Cr, 10.8 Ni, 1.88 Mn, 0.35 Nb, 0.22 Si, 0.026 C, 0.009 P, 0.001 S, balance Fe) in the solution annealed state established by tempering at 1050 °C for 30 min and terminated by water quench. Tensile deformation up to 15% plastic strain resulted in an increase in the mean positron lifetime from 124 ps to 170 ps [37].

Since the main component of these alloys is iron, we may tentatively compare our findings with the studies of Schaefer et al. [39, 40] on vacancies in iron in thermal equilibrium [39] and after 150 K electron irradiation [40], although the crystal structure of iron in the relevant temperature range is body-centered cubic. In [39] Schaefer et al. derived a migration enthalpy of $H_V^M = (1.28\pm0.25)$ eV from measurements of the wing parameter W in the ferromagnetic body-centered cubic phase. After irradiation with electrons of 3 MeV energy at 150 K with a dose of 4×10^{18} electrons cm^{-2}, Schaefer et al. [40] performed a positron annihilation line-shape analysis during isochronous annealing experiments on α-iron. A two-stage trapping model was applied as in our case. Schaefer et al. [40] found a narrow annealing stage at 550 K, which was attributed to the annealing of mono-vacancies. The data were evaluated assuming a first-order recovery kinetic $dC/dt = -Ck_0\exp(-H/k_BT)$. The evaluation of the slope in an Arrhenius plot yielded $H_V^M = 1.22$ eV with a kinetic constant of $k_0 = 10^8\,s^{-1}$. The same method applied for the evaluation of our data on deformed steel yields an activation

enthalpy of about 0.2 eV, which matches with no physically relevant effect that might contribute to the annealing of our specimens. The discrepancy that a model, which describes the annealing of irradiated specimens well, fails to derive the vacancy migration enthalpy in deformed specimens was the motivation of Dryzek et al. [6] to develop their model of diffusion in a homogeneously loaded sphere with unsaturable sinks on the surface.

The model proposed by Dryzek et al. [6] is obviously suited to determine the migration enthalpy of vacancies in deformed polycrystalline materials. It assumes a homogeneous concentration of vacancies in a spherical volume which is surrounded by grain boundaries and contains dislocations as unsaturable sinks. However, the value of $H_V^M = (0.9 \pm 0.15)$ eV found in the present investigation is significantly lower than the values so far reported in literature for Fe-Ni-Cr-based stainless steels. Dryzek et al. [6] gave a value of $H_V^M = (1.215 \pm 0.016)$ eV for stainless steel AISI 321, which has a composition very similar to AISI 316 L. However, after experience with the stability of the fit to this model made in the present investigation, it is unclear how this outstanding precision of ± 0.016 eV was obtained from a fit to only 6 *S*-parameter data. Dimitrov et al. [41] performed positron annihilation measurements at 77 K and electrical resistivity measurements on a Fe-Cr-Ni alloy in a broad range of compositions. For the alloy Fe-16 wt % Cr-12 wt % Ni, these authors obtained $H_V^M \approx (1.2 \pm 0.15)$ eV. Within the error marks, this is compatible with the present result.

For the pre-exponential factor D_0 theoretical considerations result in [1]

$$D_0 = \frac{d^2}{6} z \nu_0 \exp(S^M/k_B), \tag{5}$$

where d is the jump distance, which can be approximated by the lattice constant (3.51×10^{-10} m); z denotes the number of nearest-neighbor sites (12 for the fcc structure); ν_0 is the attempt frequency, which can be approximated by the Debye frequency (typically 10^{13} s^{-1}); and S^M denotes the vacancy migration entropy. With $\exp(S^M/k_B) \approx 1$, one obtains $D_0 \approx 2.5 \times 10^{-6}$ m^{2}s^{-1}, which agrees well with the value found for $H_V^M = 0.9$ eV (see Table 3). A typical experimental value for the pre-exponential constant obtained from thermal equilibrium studies after quenching of pure metals is 4.5×10^{-6} m^{2}s^{-1} [42].

Figure 5 illustrates the effect of the parameters on the curves calculated from Dryzek's model [6]. H_V^M, D_0 and R were varied separately, holding the other two parameters constant. The curves in Fig. 5a–c show that the strong curvature when approaching $c/c_0 = 0$ is hardly affected by any of the parameters. A curve fitted by eye would smooth this edge to better meet the measurements above 500 K, although the model describes them within the error marks. Variations of H_V^M, D_0 and R mainly shift the curves along the temperature axis. This point has already been noted by Dryzek et al. themselves [6], where an optically better fit to a simple Arrhenius type law yielded, however, activation enthalpies which were definitively too small for processes taking place in a closely packed face-centered cubic structure. An activation enthalpy as low as 0.2 eV has been reported for this type of evaluation in stainless steel AISI 321. The basic weakness of the model is the description of vacancy sinking to dislocations, since no clear picture exists on the sink strength of dislocations.

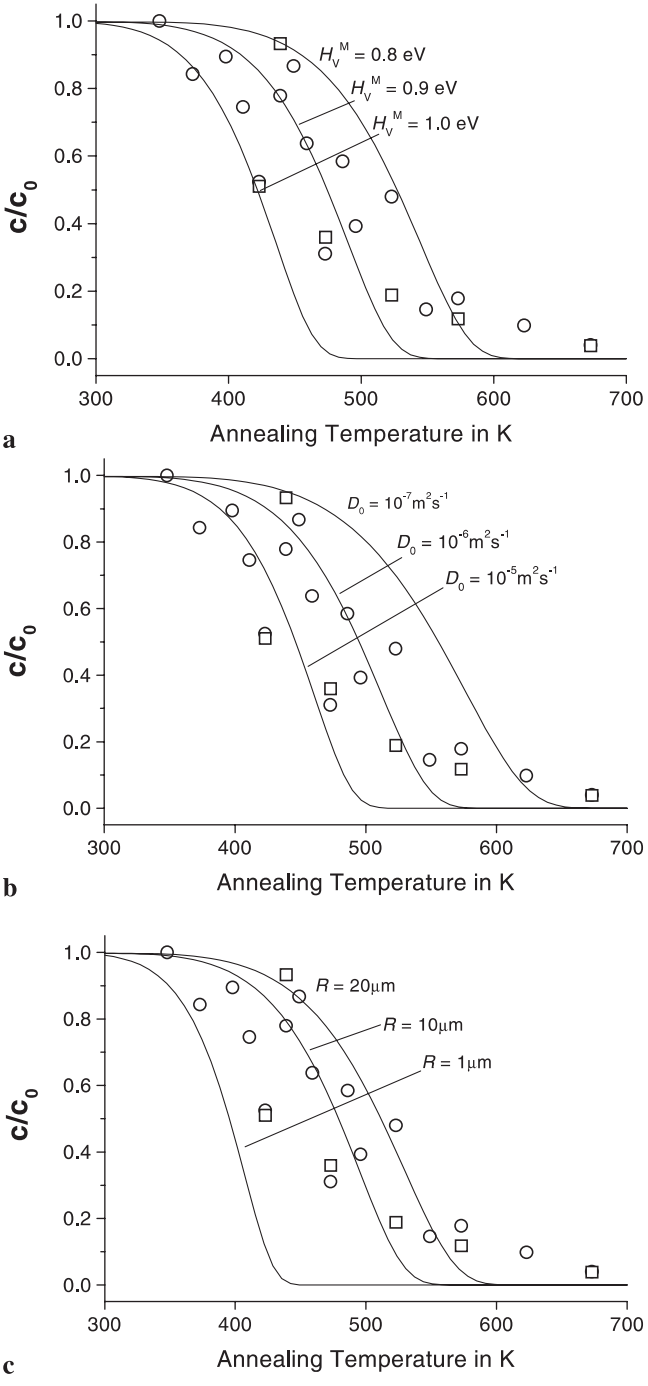

Fig. 5. Three parameters were used to fit the model of Dryzek et al. [6] to the experimental data. The effect of the migration enthalpy of vacancies H_V^M, the pre-exponential factor D_0 and the effective grain radius R were used as fit parameters. The figure illustrates their effect on the resulting curve. The constant parameters are $D_0 = 2.5 \times 10^{-6}$ m^2 s^{-1} and $R = 9$ μm in **a**, $H_V^M = 0.9$ eV and $R = 9$ μm in **b**, and $H_V^M = 0.9$ eV and $D_0 = 2.5 \times 10^{-6}$ m^2 s^{-1} in **c**

In order to check if the positron lifetime measurements yield reasonable figures for the vacancy concentrations, the specific trapping rate of positrons in vacancies is needed. Dlubek et al. determined a specific trapping rate into vacancies in a stainless steel of about 10^{15} s^{-1} [37]. In contrast to our investigations and those of Gauster et al. [16], Dlubek et al. [37] stated that they succeeded in observing positron

trapping in dislocations even at room temperature. Schaefer et al. [40] determined a trapping rate into vacancies created by 3 MeV electron irradiation at 150 K in body-centered cubic iron of $\approx 1 \times 10^{15}\,\mathrm{s}^{-1}$, which agrees well with a later investigation by Vehanen et al. [5]. These authors obtained a specific trapping rate for positrons into vacancies in α-iron of $(1.1 \pm 0.2) \times 10^{15}\,\mathrm{s}^{-1}$. Considering further typical trapping rates into vacancies in face-centered cubic materials derived by Mantl and Triftshäusser of $4.3 \pm 0.8 \times 10^{14}\,\mathrm{s}^{-1}$ [43] and by McKee et al. of $8.6 \times 10^{14}\,\mathrm{s}^{-1}$ [44] on copper, we use a value of $10^{15}\,\mathrm{s}^{-1}$ in the following calculations. All these values agree well with recent absolute determination of the trapping rates of positrons into vacancies in intermetallic FeSi and FeAl compounds by Broska et al. [45]. These authors combined positron-annihilation with differential dilatometric measurements on the same compounds to determine the absolute concentration of vacancies [46]. In $D0_3$ FeSi, the trapping rate was concentration dependent, rising from $2.9 \times 10^{14}\,\mathrm{s}^{-1}$ in $Fe_{82}Si_{18}$ to $6.6 \times 10^{14}\,\mathrm{s}^{-1}$ in $Fe_{76}Si_{24}$. In the B2-ordered $Fe_{65}Al_{35}$ a high trapping rate of $5.6 \times 10^{15}\,\mathrm{s}^{-1}$ was found [45].

A rough estimate of the vacancy densities after the thickness reduction of the slabs can be obtained applying the model of Saada [47]:

$$C_\mathrm{V} = \frac{1}{2}\frac{\beta}{G}\int_0^\varepsilon \sigma \,\mathrm{d}\varepsilon\,, \tag{6}$$

where β is a constant which can be approximated according to van den Beukel as 0.06 [48]. G denotes the shear modulus of type 316 L stainless steel, which is 75.8 GPa [24]. σ denotes the flow stress of the specimen, which increases with the plastic strain ε. For simplicity and lacking knowledge of the stress–strain curve for the compression test, the integration was approximated by $1/2 \cdot \sigma_\mathrm{end} \cdot \varepsilon_\mathrm{end}$, where σ_end denotes the the maximum registered stress of 700 MPa and 1175 MPa for a thickness reduction to ε_end of 0.1 and 0.2, respectively. This crude estimate yields vacancy concentrations of $C_\mathrm{V} = 1.4 \times 10^{-5}$ and 4.7×10^{-5} for a 10% and 20% thickness reduction, respectively. These figures may be compared with the vacancy concentration,

$$C_\mathrm{V} = \frac{1}{\tau_\mathrm{L}\mu_\mathrm{V}}\left(\frac{\tau - \tau_\mathrm{L}}{\tau_\mathrm{V} - \tau}\right)\,, \tag{7}$$

calculated from the two-stage trapping model [29, 30]. With a specific trapping rate of positrons in vacancies of $\mu_\mathrm{V} = 1 \times 10^{15}\,\mathrm{s}^{-1}$, one obtains initial vacancy concentrations after thickness reduction of 1.7×10^{-5} and 3.8×10^{-5}, respectively. Both figures agree well with the above estimate based on the model of Saada [47]. With the preceding values, one obtains as vacancy concentration due to machining, giving rise to a mean positron lifetime of 130 ps, a value of $C_0 \approx 5 \times 10^{-6}$. This figure has to be considered as an average value in the depth probed by positrons. From the accuracy of the mean positron lifetime of $\Delta\tau \pm 3$ ps, we can derive the sensitivity limit of the present measurements, i.e., the minimum concentration of vacancies that can be distinguished from the defect-free lattice. Using $\tau_\mathrm{V} = 175$ ps and $\tau_\mathrm{L} = 105$ ps in (7), a detection threshold of $C_\mathrm{limit} \approx 4 \times 10^{-7}$ is obtained. Both values seem quite reasonable.

With a mean grain size of 40 μm, the present positron lifetime measurements average over a large number of grains. The positrons emitted from a $^{72}Se/^{72}As$ generator exhibit a penetration depth in steel of about 300 μm and 500 μm for the maximum energies of 2.5 MeV and 3.3 MeV, respectively. This has been calculated for positrons with the most probable energy in the spectra, which is about 1/3 of the maximum energy. The calculation already takes into account a mean energy loss of 150 keV for the passage of the plastic scintillator and the aluminum foil shielding the start detector from daylight. Hence, the strength of the present method is to probe the bulk properties of a material. This makes this positron especially useful for non-destructive testing purposes.

The profile of the positron-annihilation line shape parameters across the cross-sectional area of a specimen shows that the effect of machining is detectable up to 5 mm below the surface. With the sensitivity of positron annihilation, this is rather bulk than surface damage. Figure 4 demonstrates that damage profiling by microhardness measurements, favorably used in engineering, is rather insensitive in this case.

From the positron line-shape profile and the microhardness profile before and after an annealing at 350 °C for 20 h, one may unambiguously conclude that the annealing effectively removed the positron traps, whereas the dislocation microstructure which determines the mechanical behaviour was not significantly affected. This finding confirms our assumption that dislocations are shallow positron traps and do not trap positrons at room temperature.

4 Conclusions

The model of Dryzek et al. [6] has successfully been applied to determine the vacancy migration enthalpy in stainless steel AISI 316 L from isochronous annealing experiments on slabs deformed in compression. A migration enthalpy of $H_\mathrm{V}^\mathrm{M} = (0.9 \pm 0.15)$ eV was obtained.

At room temperature the dominating positron traps in stainless steel AISI 316 L are single vacancies and there is no evidence for direct trapping of vacancies to dislocations. Positron-lifetime measurements on deformed specimens at room temperature are sensitive to plastic deformation via single vacancies produced by dislocations processes. Consequently, the sensitivity of positron annihilation to plastic deformations is lost by annealing of the material in a temperature range where vacancies become mobile.

The machining of stainless steel leads to a deformation of the material which can be detected by positron annihilation up to 5 mm below the machined surface.

Acknowledgements. S. Hansen-Ilzhöfer acknowledges support from the European Commission by granting a Marie Curie research Fellowship (contract number FMBICT983002) under the programme Training and Mobility of Researchers.

References

1. P. Erhardt: In *Landolt-Börnstein, Numerical Data and Functional Relationships in Science and Technology, Group III: Crystal and Solid State Physics,* Vol. 25 *Atomic* Defects *in Metals*, ed. by H. Mehrer (Springer-Verlag, Berlin, Heidelberg 1990) p. 88, p. 345

2. W. Triftshäuser, H. Matter, J. Winter: Appl. Phys. A **28**, 179 (1982)
3. Metals Handbook 9th edn., Vol. 3: *Properties and Selection – Stainless Steels, Tool Materials and Special-Purpose Metals* (American Society for Metals, Metals Park, Ohio 1980)
4. B.D. Sharma, K. Sonneberg, G. Antesberger, W. Kesternich: Philos. Mag. A **37**, 777 (1978)
5. A. Vehanen, P. Hautojärvi, J. Johansson, J. Yli-Kauppila, P. Moser: Phys. Rev. B **25**, 762 (1982)
6. J. Dryzek, C. Wesseling, E. Dryzek, B. Cleff: Mater. Lett. **21**, 209 (1994)
7. H. Mehrer: In *Landolt-Börnstein, Numerical Data and Functional Relationships in Science and Technology, Group III: Crystal and Solid State Physics,* Vol. 26 Diffusion in Solid Metals and Alloys, ed. by H. Mehrer (Springer-Verlag, Berlin, Heidelberg 1991) p. 6
8. J. Dryzek: Mater. Sci. Forum **255-257**, 533 (1997)
9. S. Hansen, U. Holzwarth, M. Tongbhoyai, T. Wider, K. Maier: Appl. Phys. A **65**, 47 (1997)
10. A. Barbieri, S. Hansen-Ilzhöfer, A. Ilzhöfer, U. Holzwarth: Appl. Phys. Lett. **77**, 1911 (2000)
11. T. Wider, S. Hansen, U Holzwarth, K. Maier: Phys. Rev. B **57**, 5126 (1998)
12. T. Wider, K. Maier, U. Holzwarth: Phys. Rev. B **60**, 179 (1999)
13. H. Häkkinen, S. Mäkinen, M. Manninen: Phys. Rev. B **41**, 12 441 (1990)
14. Y. Kamimura, T. Tsutsumi, E. Kuramoto: Phys. Rev. B **52**, 879 (1995)
15. Y. Kamimura, T. Tsutsumi, E. Kuramoto: J. Phys. Soc. Jpn. **66**, 3090 (1997)
16. W.B. Gauster, W.R. Wampler, W.B. Jones, J.A. van den Avyle: In Proceedings of the 5th International Conference on Positron Annihilation, ed. by R.R. Hasiguti, K. Fujiwara (Japan Inst. of Metals, Sendai 1979) p. 125
17. Y.-K. Park, J.T. Waber, M. Meshii, C.L. Snead, Jr., C.G. Park: Phys. Rev. B **34**, 823 (1986)
18. C. Hidalgo, G. Gonzáles-Doncel, S. Linderoth, J. San Juan: Phys. Rev. B **45**, 7017 (1992)
19. E. Hashimoto: J. Phys. Soc. Jpn. **62**, 552 (1993)
20. E. Hashimoto, M. Iwami, Y. Ueda: J. Phys.: Condens. Matter **6**, 1611 (1994)
21. K. Petersen, I.A. Repin, G. Trumpy: J. Phys.: Condens. Matter **8**, 2815 (1996)
22. L. Pryce, K.W. Andrews: J. Iron Steel Inst. **196**, 415 (1960)
23. *Annual Book of ASTM Standards, Metals Test Methods and Analytical Procedures,* Vol. 03.01 (American Society for Testing and Materials, Philadelphia, PA 1992)
24. A.E. Waltar, A.B. Reynolds: *Fast Breeder Reactors* (Pergamon Press, New York 1981)
25. R.W. Siegel: J. Nucl. Mater. **69–70**, 117 (1978)
26. T.M. Wang, B.Y. Wang, S.H. Zhang, M. Doyama: Mater. Sci. Forum **105–110**, 1321 (1992)
27. B. Somieski, T.E.M. Staab, R. Krause-Rehberg: Nucl. Instrum. Meth. Phys. Res. A **381**, 128 (1996)
28. J. Crank: *The Mathematics of Diffusion* (Oxford University Press, London 1956)
29. B. Bergersen, M.J. Stott: Solid State Comm. **7**, 1203 (1969)
30. D.C. Connors, R.N. West: Phys. Lett. **30**A, 24 (1969)
31. M. Haaks, K. Bennewitz, H. Bihr, U. Männig, C. Zamponi, K. Maier: Appl. Surf. Sci. **149**, 207 (1999)
32. H. Greif, M. Haaks, U. Holzwarth, U. Männig, M. Tongbhoyai, T. Wider, K. Maier, J. Bihr, B. Huber: Appl. Phys. Lett. **71**, 2115 (1997)
33. A.K. Koul: Metal Sci. **16**, 591 (1982)
34. Metals Handbook 9th edn., Vol. 4: Heat Treating (American Society for Metals, Metals Park, Ohio 1980)
35. C. Lopes Gil, A.P. de Lima, N. Ayres de Campos, P. Sperr, G. Kögel, W. Triftshäuser: Rad. Eff. **112**, 111 (1990)
36. J.H. Hartley, R.H. Howell, P. Asoka-Kumar, P.A. Sterne, D. Akers, A. Denison: Appl. Surf. Sci. **149**, 204 (1999)
37. G. Dlubek, A. Sourkov, S. Depetasse, N. Meyendorf: In Proceedings of the 20th RisøInternational Symposium on Materials Science: Deformation-Induced Microstructures: Analysis and Relation to Properties, ed. by J.B. Bilde Sørensen, J.V. Carstensen, N. Hansen, D. Juul Jensen, T. Leffers, W. Pantleon, O.B. Pedersen, G. Winther (RisøNational Laboratory, Roskilde 1999), p. 305
38. H.E. Schaefer: In Proceedings of the European Meeting on Positron Studies of Defects, Wernigerode Vol. 1, Part 1, PL-3 (Martin-Luther-Universität, Halle-Wittenberg and Zentralinstitut für Kernforschung, Rossendorf 1987)
39. H.-E. Schaefer, K. Maier, M. Weller, D. Herlach, A. Seeger, J. Diehl: Scripta Metall. **11**, 803 (1977)
40. H.-E. Schaefer, P. Valenta, K. Maier: In Proceedings of the 5th International Conference on Positron Annihilation, ed. by R.R. Hasiguti, K. Fujiwara (Japan Inst. of Metals, Sendai 1979) p. 509
41. C. Dimitrov, A. Benkaddour, O. Dimitrov, C. Corbel, P. Moser: Mater. Sci. Forum **15–18**, 1275 (1987)
42. R.W. Baluffi: J. Nucl. Mater. **69–70**, 240 (1978)
43. S. Mantl, W. Triftshäuser: Phys. Rev. B **17**, 1645 (1978)
44. B.T.A. McKee, S. Saimoto, A.T. Stewart, M.J. Stott: Can. J. Phys. **52**, 759 (1978)
45. A. Broska, J. Wolff, M. Franz, Th. Hehenkamp: Intermetallics **7**, 259 (1999)
46. R. Kerl, J. Wolff, Th. Hehenkamp: Intermetallics **7**, 301 (1999)
47. G. Saada: Acta Metall. **9**, 166 (1961); ibid.: Acta Metall. **9**, 965 (1961)
48. A. van den Beukel: In *Vacancies and Interstitials in Metals*, ed. by A. Seeger, D. Schumacher, W. Schilling, J. Diehl (North-Holland, Amsterdam 1970) p. 427